Evaporative Cooling with a Wet Fabric Blanket for Non-Refrigerated Horticultural Produce Transport: An Experimental Study

Nattawut Chaomuang, Onrawee Laguerre, Suriyan Supapvanich, D. Flick, Steven Duret

Evaporative cooling with a wet fabric blanket for non-refrigerated horticultural produce transport: An experimental study

Nattawut Chaomuang[a,*], Onrawee Laguerre[b], Suriyan Supapvanich[c], Denis Flick[d] and Steven Duret[b]

[a] Department of Food Engineering, School of Engineering, King Mongkut's Institute of Technology Ladkrabang, Bangkok, 10520, Thailand

[b] Université Paris-Saclay, INRAE, FRISE, 92761, Antony, France

[c] Department of Agricultural Education, School of Industrial Education and Technology, King Mongkut's Institute of Technology Ladkrabang, Bangkok, 10520, Thailand

[d] Université Paris-Saclay, INRAE, AgroParisTech, UMR SayFood, 91120, Palaiseau, France

***Corresponding author:** Nattawut Chaomuang, e-mail: nattawut.ch@kmitl.ac.th

Abstract

Due to the high cost of mechanical refrigeration, Evaporative Cooling (EC) can be an alternative technology for small farmers in developing countries, such as Thailand. This study aimed to experimentally investigate the performance of EC using a wet fabric blanket. A real-scale cargo chamber, commonly used in Thailand, was constructed, and equipped with axial fans to simulate airflow during transportation. Two pallets of test products (hollow plastic balls) were loaded into the cargo and covered with the wet blanket. During the experiment, the inlet air velocities varied from 0.8 $m \cdot s^{-1}$ to 3.6 $m \cdot s^{-1}$ while the constant climate conditions were maintained (29-30 °C and 70-73 %RH). The air and product temperatures and air relative humidity were measured every minute for three hours using thermocouples and hygrometers, respectively. This EC method allowed the air temperature decrease by approximately 3-4 °C. When the inlet air velocity decreased, a lower temperature reduction was observed. The quality preservation performance was also evaluated based on lettuce mass loss. Lower mass loss was observed for the product stored inside the cargo chamber (< 6%) compared to those outside (8-10%). This study suggests the potential use of a wet blanket as an EC cooling medium for a short-distance transport to enhance the cold chain performance in Thailand.

Keywords: Cold Chain; Food Loss; Passive Cooling; Temperature; Tropical Climate; Vegetable.

Nomenclature

A_c	cross-sectional area (m^2)
c	regression coefficient (-)
c_p	specific heat capacity ($J \cdot kg^{-1} \cdot K^{-1}$)
C	moisture concentration ($kg \cdot m^{-3}$)
CR	cumulative respired CO_2 concentration ($g \cdot kg^{-1}$)
DL	defective loss percentage (%)
e	load thickness (m)
h	heat transfer coefficient ($W \cdot m^{-2} \cdot K^{-1}$)
J_v	evaporative flux ($kg \cdot m^{-1} \cdot s^{-1}$)
k	mass transfer coefficient ($m^2 \cdot s^{-1}$)
L_v	Latent heat of evaporation ($kJ \cdot kg^{-1}$)
m	mass (kg)
$\dot{m}$	mass flow rate ($kg \cdot s^{-1}$)
M	molar mass ($g \cdot mol^{-1}$)
ML	mass loss percentage (%)
p_v	partial vapor pressure (Pa)
R_a	coefficient specific to a product (dimensionless)
R_u	universal gas constant ($m3 \cdot Pa \cdot mol^{-1} \cdot K^{-1}$)
R_{CO2}	respired CO_2 rate ($g \cdot kg^{-1} \cdot h^{-1}$)
S	total surface area of cargo (m^2)
S_{ext}	surface of cargo in contact with external air (m^2)
T	dry-bulb temperature (DBT, °C)
T'	wet-bulb temperature (WBT, °C)
$\bar{u}$	average velocity ($m \cdot s^{-1}$)
V	volume (m^3)
$\dot{V}$	volumetric flow rate ($m^3 \cdot s^{-1}$)
α	coefficient specific to a product (dimensionless)
β	special functions (-)
ε_{sat}	saturation effectiveness (%)
ρ	density ($kg \cdot m^{-3}$)

τ	characteristic time (s)
φ	relative humidity (%)
ω	humidity ratio (kg of water vapor · kg^{-1} of dry air)

Subscripts

a	air
df	defect
ext	external
f	fabric
in	inlet
l	load
p	product
sat	saturation
0	initial

1. Introduction

Road transport is the most common mode of freight transport in Thailand, accounting for almost 80% of the total domestic freight volume (Sathapongpakdee, 2022). Pickup trucks are typically used to distribute small volumes of goods inside the country. The total number of registered pickup trucks was around 7 million units while that of other registered trucks was only about 1.2 million units (DLT, 2022). The pickup trucks for freight transport can be classified into three types according to bed configurations namely fence bed, dry cargo chamber, and refrigerated cargo chamber. Because of its simple structure, relatively low capital and operational costs, the first two types are broadly used by most small and medium enterprises (SMEs) in food and agriculture sectors in Thailand while the one of refrigerated cargo chamber is much less (DLT, 2023).

Storage temperature and humidity are known to be significant factors affecting quality deterioration and postharvest lifetime of horticultural produce (Han et al., 2021). Uninterrupted series of refrigeration units in supply chains or "cold chains" is of importance to maintain optimal temperature until consumption (Kim et al., 2015). In 2013, International Institute of Refrigeration (IIR) estimated that 13% of food produced in the world is lost due to a lack of refrigeration (IIR, 2020). In this regard, transport by non-refrigerated pickup truck can be problematic.

In Thailand, the majority of agricultural production is carried out by small-scale farmers who usually cultivate approximately four hectares of land (Kwanmuang et al., 2020) while their annual incomes are often below the national poverty line (Chantarat et al., 2018). Despite their understanding of the negative impacts of inadequate temperature control, mechanical refrigeration is not economically affordable for them. Furthermore, the benefits of refrigeration, such as increased selling price due to high quality and reduced loss, may not outweigh the expenses incurred from installing and operating the refrigeration within a reasonable timeframe due to economy of scale. Finding an alternative low-cost technology becomes obvious.

Evaporative Cooling (EC), a simultaneous heat and mass transfer process, has been implemented since ancient times and is increasingly popular in many cooling applications including horticultural produce storage (Nkolisa et al., 2018). When water is in contact with warm and dry surrounding air, the water evaporates while the air becomes colder and humidified. The driving forces of water evaporation are the ambient temperature and vapor partial pressure differences (Xuan et al., 2012). Air temperature can be decreased up to the difference between the dry-bulb and wet-bulb temperatures, indicating the air capacity to hold moisture (Liu et al., 2020). The effective temperature decrease divided by the maximum temperature decrease is referred to "saturation effectiveness" (Tejero-González and Franco-Salas, 2021). Thailand is a warm and humid country with temperature range 20-40 °C and relative humidity 60-80 % (TMD, 2020). Hence, low saturation effectiveness is expected for the EC implementation for horticultural produce storage in the country (Defraeye et al., 2023). Nevertheless, small temperature drops caused by EC are more adapted to short-distance transport of tropical fruits and vegetables with optimal temperature range of 10-13 °C as too low temperature engenders chilling injury. Moreover, the increase in air relative humidity would also limit the weight loss of the produce, which is related to its marketability. Vala and Joshi (2010) demonstrated the application feasibility under Indian climate conditions with a reduced-scale cargo chamber without load. Depending on the pad materials, the achieved air temperature drops varied between 2 and 12 °C, corresponding to the saturation effectiveness of 30-90 %.

Generally, the EC requires a water supply system (pump, piping, and water reservoir) installed in a cargo chamber, but it decreases loading capacity. In this regard, the EC by using wet fabric blanket was proposed in this study. Chopra et al. (2022) evaluated the performance an EC storage with wet nylon felt walls under Indian climate conditions. On average over 24-hour period, a temperature difference of about 5 °C between the stored products and ambient temperature was achieved. Guo (2016) evaluated the EC effect of different types of fabrics (cotton, wool, and cotton-based linen) under real transport with different speeds (0-70 $km \cdot h^{-1}$). At the highest speed, the EC utilizing the wet cotton was able to lower the air temperature from 32 °C (40 %RH) to 18 °C (87 %RH) after 8 minutes. The finding showed the potential of the cooling technique. Our previous study also confirmed this result (Chaomuang and Flick, 2022). However, the obtained results were based on the experiments in a small-scale container (≈ 0.06 m^3) with no loads. A question is whether this cooling technique is still satisfactory in a cargo chamber with a real size of 120 folds higher (≈ 7.2 m^3 for a typical dry cargo chamber hauled by a pickup truck). The present study aimed to evaluate experimentally the cooling performance of the EC system using a wet fabric blanket covering the pallets of loads in a full-scale test cargo chamber. First, the air velocity inside the cargo chamber was characterized, followed by the measurement of the air and hollow sphere temperatures. Next, the effect of airflow rate on the reduction of air and load (surface) temperatures was studied. Simplified heat and mass transfer models were developed to interpret the load temperature evolution from the inlet to the outlet positions at different air velocities. Finally, the impact of temperature and relative humidity on lettuce weight loss at different positions was investigated. The knowledge acquired in this study would provide practical suggestions for smallholder farmers to transport their products at a better condition while compromising their incomes to the least extent. This would also allow a decent short-term solution to improve cold chain logistic in Thailand before the infrastructure is fully established.

2. Materials and methods

2.1 Experimental apparatus

A test cargo chamber was constructed with the same scale as the one of pickup trucks typically used for land transport in Thailand. Its internal dimensions were 1.78 m (width) × 2.35 m (length) × 1.76 m (height), corresponding to 7.36 m^3 loading capacity (**Fig. 1**). Its walls were made of thin aluminum sheets (thickness = 0.6 mm) without thermal insulation. It had one air inlet (1.2 m × 0.3 m) on the front wall and two outlets (0.4 m × 0.4 m) on the rear wall. A suction axial fan (Weiguang YWF4D-350S, 140 W, 2500 $m^3 \cdot h^{-1}$) was mounted on each outlet to induce airflow across the cargo chamber. In practice, on one hand, such fans can be installed inexpensively to ensure a continuous airflow throughout the cargo chamber, on the other hand, if a cargo chamber without fans is used, there is still an airflow throughout the cargo chamber when the truck is travelling on the road.

Extending ducts (length = 0.3 m) were installed at the inlet and the outlets to enable the measurement of the temperature and relative humidity of mixed air at these locations. The fans were connected in parallel to a variable-frequency drive (Jaden JZ-100) to control the fan speed by varying the electrical frequency.

The cargo chamber was installed in a laboratory test room where the air temperature and the relative humidity during all experiments varied in the range of 29-30 °C and 70-75 %RH, respectively, which represent real climatic conditions in Thailand.

Two pallets of loads were placed inside the cargo chamber. Each pallet contained 42 perforated polypropylene baskets (mass = 660 g, volume = 22.7 L) evenly distributed into 6 stacks (i.e., 7 baskets per stack). Each basket was filled with 35 hollow spheres (mass = 8.5 g, outer diameter = 72 mm, thickness = 0.3 mm) made of low-density polyethylene (**Fig. 2a**) to represent the bulk package of sphere-shaped horticultural produce such as tomatoes, oranges, etc. Since these spheres provide similar resistance to airflow, the same airflow pattern as in real conditions can be achieved. In a first approach, if respiration heat and water loss of product can be neglected, at steady state, the temperatures (air and load surface) measured in these laboratory conditions are representative of real conditions. Nevertheless, since the thermal inertia of these hollow plastic spheres is very low compared to real products, the transient temperature evolutions are much faster than in real conditions.

The fabric blanket used is made of acrylic felt due to high water retention capacity (3 kg water/kg dry mass), availability in local markets, and cheap price. Seven acrylic felts (thickness = 5 mm) were patched together to assemble a large blanket (420 $g \cdot m^{-2}$) which can perfectly cover two pallets of loads (**Fig. 2c**). The wet blanket was prepared by spraying it with tap water until it was soddened (~20 L).

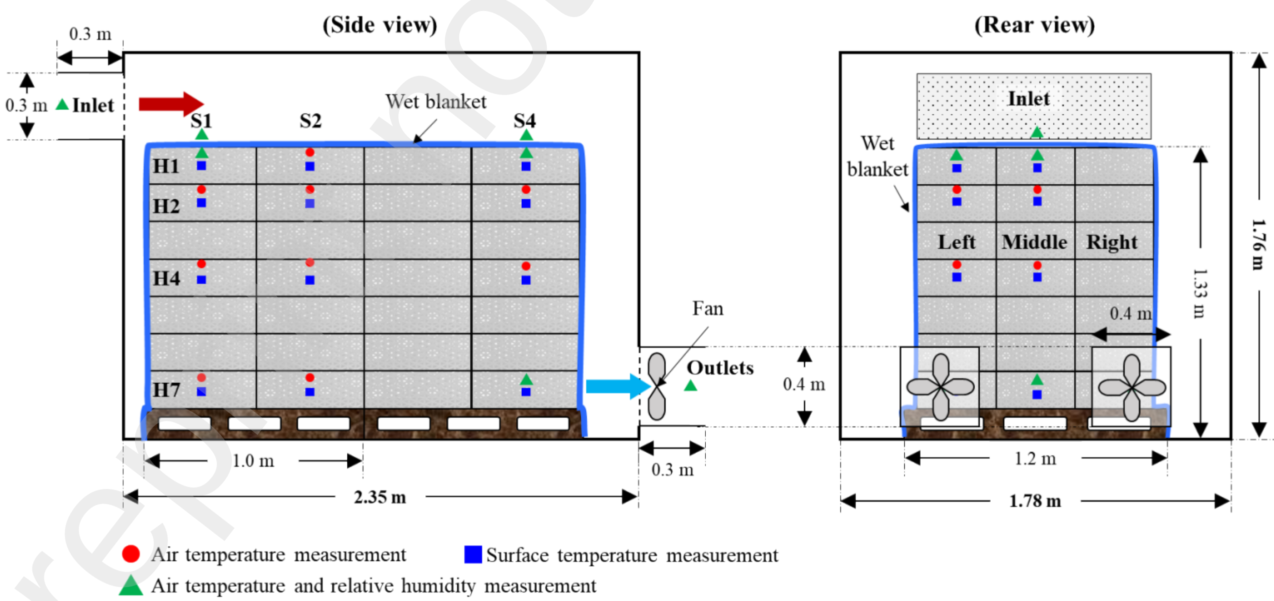

Fig. 1 Schematic of a test cargo chamber and the experimental setup for temperature and relative humidity measurements.

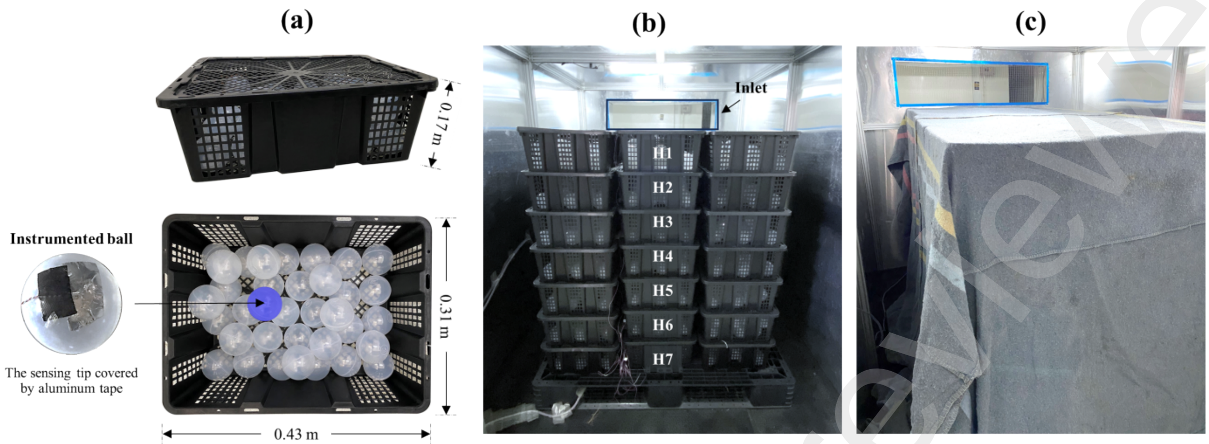

Fig. 2 (a) Dimensions of a basket loaded with hollow plastic balls, (b) photograph of the basket arrangement in a cargo chamber, and (c) photograph of the baskets covered by a wet blanket.

2.2 Velocity measurement

2.2.1 Determination of air inlet and outlet mass flow rates

A hot-wire anemometer (Testo 440, accuracy ±0.03 m·s^{-1} in the measuring range of 0-20 m·s^{-1}) was used to measure air velocity at the inlet and the two outlets under five fan speed conditions. The fan speed was varied by adjusting the input power frequency to 10, 20, 30, 40, and 50 Hz. The measurements were conducted at 55 points across the inlet and 16 points across each outlet. At each measuring point, the air velocity was recorded every ten seconds for two minutes, and the time-averaged values were determined. The mass flow rates ($\dot{m}_a$) were then calculated based on the averaged velocity of all measuring points ($\bar{u}_a$):

$$\dot{m}_a = \rho_a A_c \bar{u}_a \tag{1}$$

where ρ_a is the air density (1.16 kg·m^{-3} at 30 °C) and A_c is the cross-sectional area of the inlet (0.36 m^2) or of the outlets (0.16 m^2).

2.2.2 Characterization of airflow in the cargo chamber

Air velocity measurement in the cargo chamber was also conducted to describe the airflow around the pallets covered by the blanket at the different fan speeds explained in the previous section. As depicted in **Fig. 3**, there were 15 points for the measurements on the left (z = 0.3 m) and the right (z = 1.5 m) planes, and 9 points for the measurements on the middle plane (z = 0.9 m). The sensor was 2-cm distance from the blanket. The hot-wire anemometer was installed on a portable stand to facilitate sensor displacement. At each point, the air velocity was measured in two directions (x and y) by changing the orientation of the sensor to obtain two-dimensional (2D) velocity fields. The recording intervals and duration for each measurement were ten seconds and two minutes, respectively. The velocity magnitude at each point was determined from:

$$\overline{u}_a = \sqrt{\overline{u}_{a,x}^2 + \overline{u}_{a,y}^2} \tag{2}$$

The 2D vector fields were then plotted using MATLAB software (version R2021b).

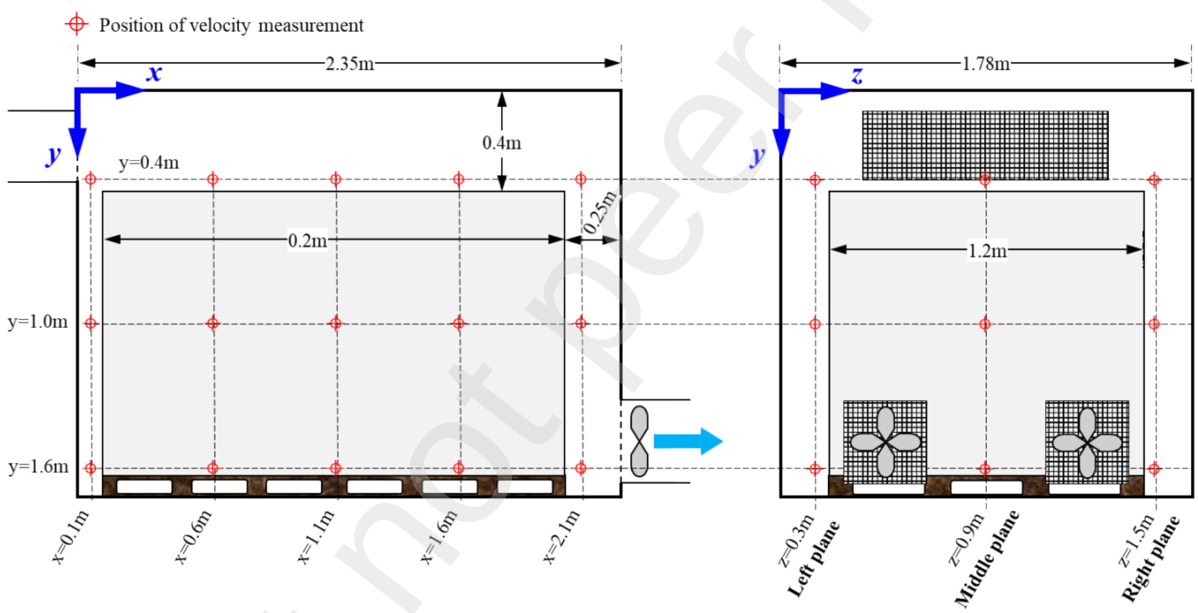

Fig. 3 Experimental setup for air velocity measurement.

2.3 Temperature and relative humidity measurement

Calibrated T-type thermocouples (diameters = 0.3 mm, accuracy ±0.2 °C) were used to measure the air and the surface temperatures of the loads in the center of the baskets at four heights: H1 (top), H2, H4, and H7 (bottom) of stacks S1, S2, and S4 in the middle of the cargo chamber and of stacks S1 and S4 on the left of the cargo chamber (red circles and blue squares in **Fig. 1**). Aluminum tape was used to attach a thermocouple to a load surface (**Fig. 2a**). All thermocouples were connected to a data acquisition unit (Keysight 34972A) and were set to record the temperature every minute for a duration of at least three hours (representation of short-distance transport duration). Thermo-hygrometers (Testo 174H, accuracy ±0.5 °C and ±3 %RH) were also used to measure the air temperature and the relative humidity in some baskets (S1H1, S4H1, and S4H7, green triangles in **Fig. 1**). The recording intervals for these thermo-hygrometers were every minute.

To investigate the air and surface temperature distributions in the pallets, the inlet air velocity was first set to its maximum corresponding to the frequency of 50 Hz. A series of experiments was subsequently carried out to investigate the influence of inlet air velocity (10 Hz, 20 Hz, 30 Hz, and 40 Hz). Two replications were conducted for each inlet air velocity.

The saturation effectiveness (ε_{sat}) of EC was calculated using the following equation (Tejero-González and Franco-Salas, 2021):

$$\varepsilon_{sat} = \frac{T_{a,in} - T_{a,k}}{T_{a,in} - T'_{a,in}} \times 100\% \qquad (3)$$

where $T_{a,in}$ and $T'_{a,in}$ are the dry-bulb and wet-bulb inlet air temperatures (°C), respectively, and $T_{a,k}$ is the dry-bulb air temperature in a specific basket k.

An instantaneous wet-bulb air temperature (T'_a) was determined from the dry-bulb temperature and the relative humidity of the moist air using an empirical equation proposed by Stull (2011).

$$\begin{aligned} T'_a = T_a \tan^{-1}\left[0.151977(\varphi_a + 8.313659)^{0.5}\right] + \tan^{-1}(T_a + \varphi_a) - \tan^{-1}(\varphi_a - 1.676331) \\ + 0.00391838\varphi_a^{1.5}\tan^{-1}(0.023101\varphi_a) - 4.686035 \end{aligned} \qquad (4)$$

where φ_a is air relative humidity (%) and the arctangent function is in radians.

A humidity ratio (ω_a) was also calculated using the following equation (Sensirion, 2009).

$$\omega_a = 0.622 \cdot \frac{p_v}{101325 - p_v} \qquad (5)$$

where p_v is partial vapor pressure (Pa) which is given by

$$p_v = 6.112\varphi_a \exp\left(\frac{17.62T_a}{243.12 + T_a}\right) \qquad (6)$$

2.4 Evaluation of quality preservation performance

A case study with lettuce (*Lactuca sativa* L.) was conducted to investigate the preservation performance of the EC using the wet fabric blanket. Fresh lettuce was procured from a local market for each experimental day. Approximately 2 kg of lettuce with no defects (initial mass, m_0) were filled in each basket at the top and the bottom of the front (S1H1 and S1H7) and the rear stacks (S4H1 and S4H7) in the middle and the left of the cargo chamber (eight baskets in total). The other baskets remained containing plastic spheres. Three baskets of lettuce (denoted as EX1, EX2, EX3) were prepared and placed in the same room as the cargo chamber. Temperature data loggers (iButton DS1922L, accuracy ±0.5 °C) were placed in the center of all baskets loaded with lettuce to monitor product temperature throughout the experiment. Thermo-hygrometer dataloggers were also used to track air temperature and relative humidity at the inlet of the cargo chamber. The experiment was carried out with the highest inlet air velocity for 20 hours (from 11:00 AM to 8:00 AM). At the end of the experiment, the bulk mass (m) was measured, and the mass loss percentage (ML) was calculated using **Eq. (7)**.

$$ML = \frac{m_0 - m}{m_0} \times 100\% \tag{7}$$

Subsequently, defective leaves (e.g., bruises or leaf injuries) were evaluated visually and weighed for each basket (m_{df}). The defective loss percentage (DL) was then calculated using **Eq. (8)**.

$$DL = \frac{m - m_{df}}{m} \times 100\% \tag{8}$$

The same experiment was repeated to ensure the result consistency.

Apart from the two physical loss parameters (ML and DL), the cumulative respired CO_2 concentration (CR, g·kg^{-1}) was also calculated to assess the potential of the EC to prolong storage lifespan (Mahangade et al., 2020). The respired CO_2 rate (R_{CO2}, g·kg^{-1}·h^{-1}) for each time interval (1-min in our case) was calculated from the product temperature using the Arrhenius equation.

$$R_{CO2} = R_a \cdot \exp\left(\frac{-\alpha}{T_p + 273.15}\right) \quad (9)$$

where R_a and α are dimensionless coefficients specific to a product. For leaf lettuce, R_a = 0.196 and α = 5827.8 (Eriko et al., 2001). The 20-h cumulative respired CO_2 was determined by integrating the respired CO_2 rates for products stored inside and outside the cargo.

3. Results and discussion

3.1 Airflow in the cargo chamber

Inlet air velocity was almost linearly proportional to input frequency supplied to the fan (**Table 1**). The values varied from 0.8 m·s^{-1} to 3.6 m·s^{-1}, corresponding to the mass flow rate increasing from 0.34 kg·s^{-1} to 1.53 kg·s^{-1}. The air velocities at both outlets were almost identical at the same fan speed. The maximum difference in mass balance between the inlet and the outlets is of 7% at the higher fan speeds (≥ 30 Hz) where $\dot{m}_{a,in} < \dot{m}_{a,out}$. This may be explained by air entering the gaps and sensor holes on the cargo chamber walls.

In fact, reproducing the airflow throughout a cargo chamber without fans in a real transportation with, for example, a vehicle velocity of 30 km·h^{-1} (≈ 8 m·s^{-1}) necessitates a wind tunnel, which is not available in our laboratory. It should be noted that the inlet air velocity is expected to be much lower than the vehicle speed because of the pressure drop of the cargo chamber. For example, considering a singular pressure drop coefficient of about 4 (two sudden contractions/enlargements and two direction changes), the inlet air velocity is expected to be about half ($1/\sqrt{4}$) of the vehicle speed. Therefore, despite the relatively low air velocity range achieved in this study, the results can still demonstrate the potential of the EC with the wet fabric blanket.

Table 1 Air velocity and corresponding mass flow rate at different fan speeds.

Frequency	**Inlet**		**Left outlet**		**Right outlet**	
	Velocity†	Flow rate	Velocity‡	Flow rate	Velocity‡	Flow rate
(Hz)	(m·s^{-1})	(kg·s^{-1})	(m·s^{-1})	(kg·s^{-1})	(m·s^{-1})	(kg·s^{-1})
10	0.8 ± 0.2	0.34	0.9 ± 0.4	0.17	0.9 ± 0.5	0.17
20	1.6 ± 0.6	0.68	1.7 ± 0.9	0.32	1.7 ± 0.8	0.32
30	2.2 ± 0.9	0.93	2.6 ± 1.2	0.49	2.4 ± 1.2	0.45
40	2.9 ± 1.2	1.23	3.5 ± 1.5	0.66	3.5 ± 1.8	0.66

50	3.6 ± 1.5	1.53	4.3 ± 1.8	0.81	4.2 ± 2.1	0.79

[†]Average of 55 measuring points ± standard deviation. [‡]Average of 16 measuring points ± standard deviation.

Air velocity was measured at various positions around the pallets for different inlet air velocities. It was observed that the airflow on the same plane exhibited the same flow pattern for all inlet air velocities. To be concise, only the air velocity fields at different planes at three inlet air velocities (0.8, 2.2, and 3.6 $m \cdot s^{-1}$) were presented as shown in **Fig. 4**. Regardless of the inlet velocity, the high air velocity zone consistently remained above the loads ($y > 0.4$ m). When the inlet velocity was 3.6 $m \cdot s^{-1}$ (**Fig. 4c**), the air velocity in this zone ($x > 0.6$ m) ranged between 2.6 and 2.8 $m \cdot s^{-1}$ in the middle plane ($z = 0.9$ m) and between 1.2 and 2.9 $m \cdot s^{-1}$ for the lateral planes ($z = 0.3$ m and $z = 1.5$ m). Outside this zone, air velocities remained below 1.0 $m \cdot s^{-1}$ for all planes. These findings suggested that the EC effect in the high velocity zone (large proportion of air flow) would be relatively high compared to the other positions. When the inlet velocity decreased from 3.6 $m \cdot s^{-1}$ to 2.2 $m \cdot s^{-1}$ (**Fig. 4b**) and 0.8 $m \cdot s^{-1}$ (**Fig. 4a**), the air velocities in this zone dropped by 40-50% and 80-85%, respectively.

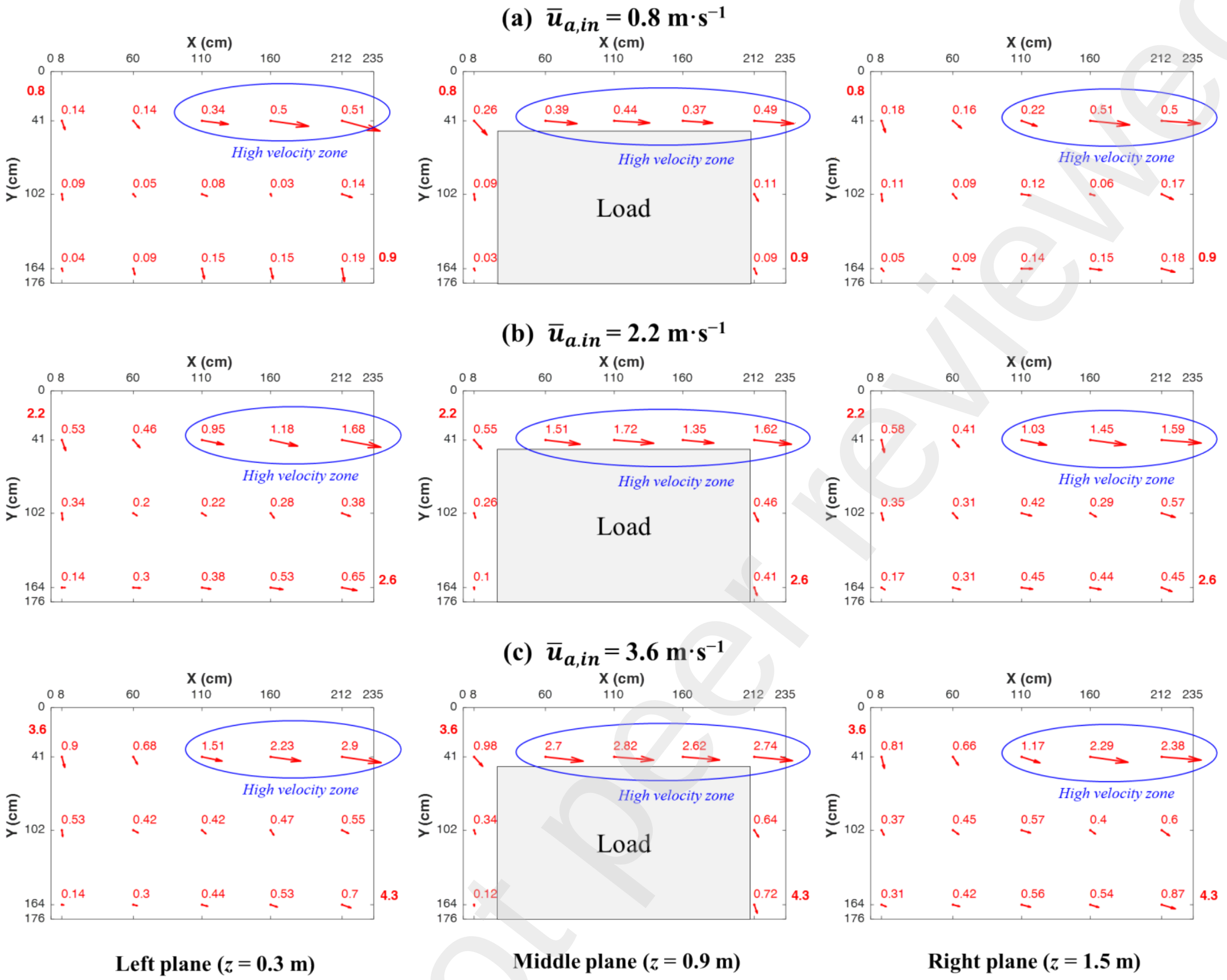

Fig. 4 Air velocity fields at different planes in the cargo chamber at the three inlet velocities ($\bar{u}_{a,in}$): (a) 0.8 m·s^{-1}, (b) 2.2 m·s^{-1}, and (c) 3.6 m·s^{-1}. Bold numbers outside the plot area indicate the inlet velocity (left) and left outlet velocity (right).

3.2 Temperature distribution in the pallets

The lowest achievable air temperature through EC is determined by the wet-bulb temperature of the ambient air. Consequently, the EC potential in this study is expected to be constrained due to the high humidity environment (29.8 ± 0.2 °C and 70.3 ± 1.6 %RH, corresponding wet-bulb temperature = 25.5 °C). **Fig. 5** shows air and load surface temperature variations at various positions in the cargo chamber when the inlet velocity was 3.6 m·s^{-1}. The air temperatures within all instrumented baskets exhibited an average reduction of 4.0 °C after 1.5 hours and subsequently remained relatively stable, with a slight variation of 0.2 °C, until the end of the experiment. These attained temperatures closely aligned with the time-averaged wet-bulb temperature of the incoming air (25.5 °C). Regarding the load surface temperature, it was observed that the change in load surface temperature did not significantly differ from the change in air temperature. This can be attributed to the low thermal inertia in this experiment (hollow plastic spheres). Taking into account of the mass and the heat capacity of the load (baskets and the spheres within), about 100 W was transferred from load to air at the beginning of refrigeration. This is very far from the theoretical maximum refrigeration power, for example, if the inlet air (29.8 °C, 70 % RH, 3.6 $m \cdot s^{-1}$) passes from the wet bulb temperature of 25.5 °C to 26.5 °C about 8 kW could be transferred flow load to air.

Regrading spatial variations, in the first stacks (S1) positioned both on the left (**Fig. 5a**) and in the middle (**Fig. 5b**) of the pallets, the air temperatures in the baskets at all heights showed negligible differences after 1.5 hours (< 0.5 °C). However, in the second (S2) and the last (S4) stacks, located in the middle of the pallet as depicted in **Figs. 5c** and **5e**, the air temperatures in the top baskets (H1) were relatively lower by 1.0-1.5 °C compared to those in the bottom baskets (H7). As the air traversed through the pallets, the air temperatures in the lower baskets in the subsequent stacks gradually increased, surpassing that of the front stack (S1). Conversely, the air temperatures in the top baskets of all stacks remained relatively the same. It can also be observed that the top baskets are cooled down faster during the first hour. This phenomenon can be attributed to these top baskets being in direct contact with the wet blanket, thereby benefiting from the EC effect and by the high air velocity above them.

Fig. 6 shows the variations in air relative humidity and humidity ratio at the inlet, the outlets, above the wet blanket (S1T and S4T) and, inside the three baskets on the middle stacks (S1H1, S4H1, and S4H7). The relative humidity approached 100% in the top baskets, while it was approximately 84% above the wet blanket (**Fig .6a**). A relative humidity of 91% was observed in the bottom basket. These values fall within the favorable range for the storage of various fresh fruits and vegetables. The relative humidity at both outlets appeared to be lower than that in the cargo chamber but higher than at the inlet. Indeed, the air at the outlet is a mix between the air flowing through the wet blanket and air flowing directly from the inlet. A slight increase in air temperature at the outlets also reduced the relative humidity. Nevertheless, the humidity ratios at these positions were almost the same (**Fig. 6b**).

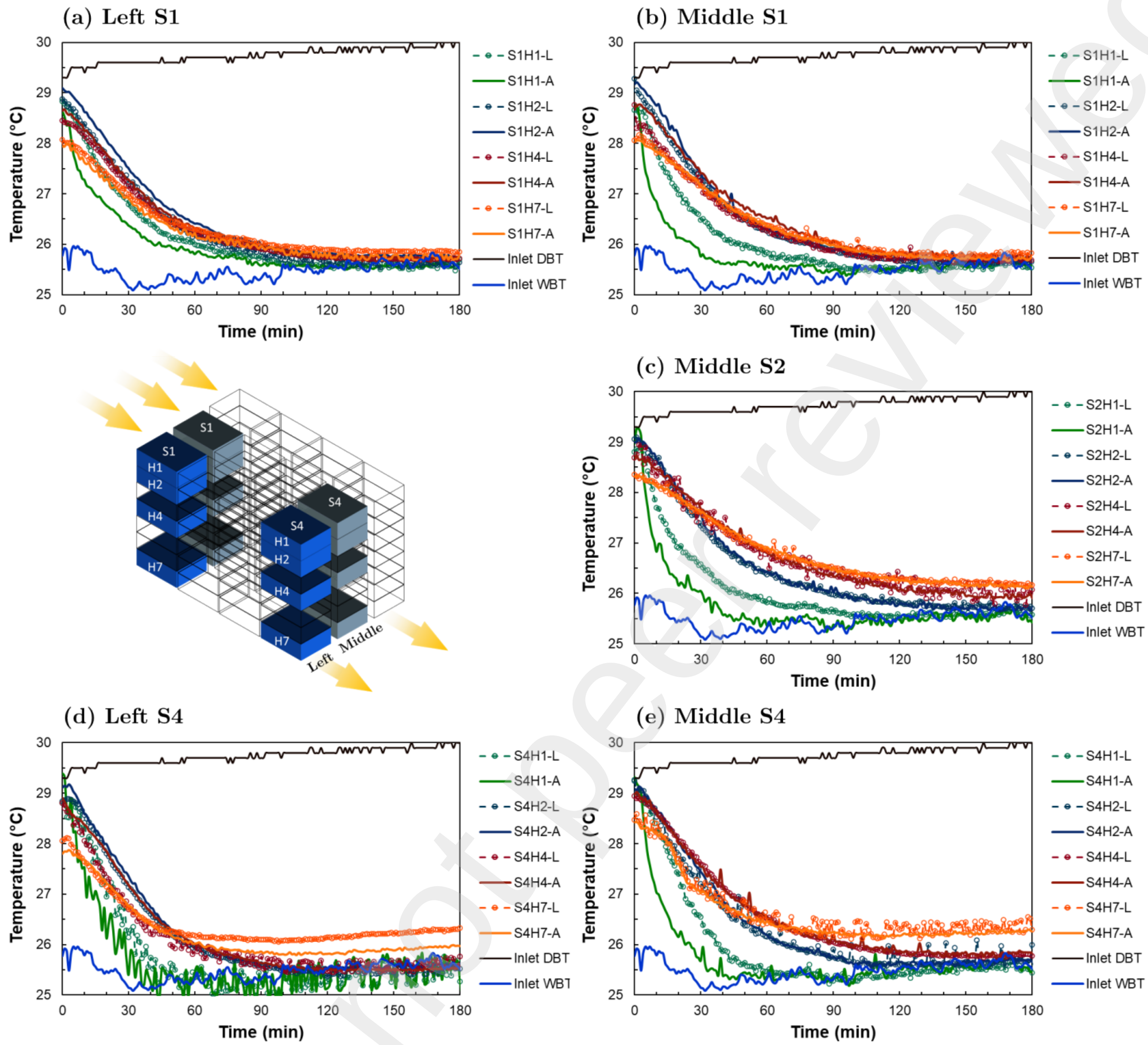

Fig. 5 Air (A) and load surface (L) temperature variations in the baskets on the left and the middle stacks ($\overline{u}_{a,in}$= 3.6 m·s^{-1} and $\overline{T}_{a,in}$ = 29.8 ± 0.2 °C).

It is noteworthy that even a minor temperature reduction associated with a slight relative humidity increase can exert a positive influence on product quality, particularly concerning moisture loss and wilting (Chaomuang et al., 2023; Defraeye et al., 2022). Ambuko et al. (2017) conducted a study revealing that leafy amaranth vegetables (*Amaranthus* spp.) experienced a substantial weight loss of nearly 50% after being stored for 5 days at ambient temperature (a maximum daytime temperature of 29 °C and a minimum nighttime temperature of 15 °C). The same authors compared the vegetable weight loss when the products were stored in two distinct storage chambers, the first one with an evaporative cooler to maintain temperatures 5–10 °C lower than ambient temperature, and the second one with a zero-energy brick cooler to maintain temperatures 1–5 °C lower than ambient temperature. They found that the weight loss was significantly reduced in the first one (7%) in comparison with the second one (10%).

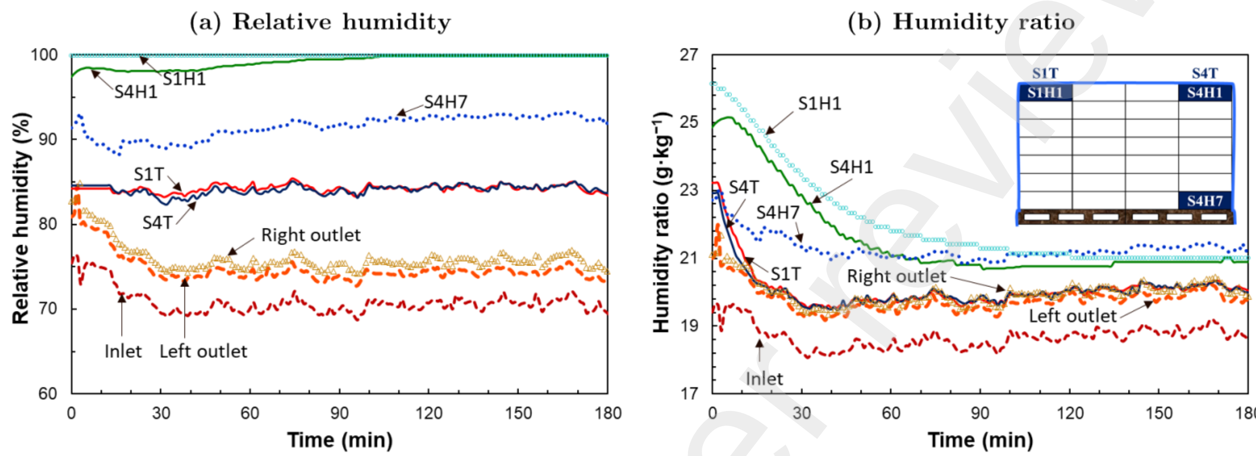

Fig. 6 Air relative humidity (a) and humidity ratio (b) variations at the inlet, the outlets, above the wet blanket (S1T and S4T) and inside the baskets (S1H1, S4H1, and S4H7) on the middle stacks ($\overline{u}_{a,in}$= 3.6 m·s^{-1}, $\overline{\varphi}_{a,in}$ = 70.3 ± 1.6 %RH, $\overline{\varphi}_{a,out\_left}$ = 74.2 ± 1.9 %RH, and $\overline{\varphi}_{a,out\_right}$ = 75.5 ± 1.9 %RH).

3.3 Influence of inlet air velocity

The temperature differentials between the inlet air and the air within the baskets in the middle plane for different air velocities are depicted in **Fig. 7**. It is evident that the most substantial temperature reductions were achieved at the highest inlet air velocity (3.6 m·s^{-1}), yielding temperature reductions ranging from 3.6 to 4.4 °C, depending on the position within the pallets. Less temperature drops were observed at lower inlet velocities. At the lowest inlet velocity (0.8 m·s^{-1}), the temperature drops were within the range of 2.4 to 3.4 °C. Remarkably, even under this condition of notably low inlet velocity, this EC technique demonstrated a saturation effectiveness of around 80% in the top baskets ($\overline{T}_{a,in} - \overline{T}'_{a,in}$= 4.1 °C). This finding was consistent with Defraeye et al. (2022) who studied the EC performance of the textile blanket filled with charcoal. They observed that the air temperature decreased by about 5 °C from the ambient temperature of 23 °C (40 %RH) even under very low airflow conditions and decreased slightly more at higher air velocity.

$\overline{T}_{a.in} = 29.5$ °C, $\overline{u}_{a.in} = 0.8$ m·s^{-1}

3.2	3.3		3.2
2.5	2.6		2.5
2.3	2.4		2.2
2.5	2.6		2.7

$\overline{T}_{a.in} = 29.9$ °C, $\overline{u}_{a.in} = 1.6$ m·s^{-1}

3.7	3.9		3.9
2.7	3.0		2.7
2.4	2.8		2.4
2.9	3.0		3.0

$\overline{T}_{a.in} = 29.1$ °C, $\overline{u}_{a.in} = 2.2$ m·s^{-1}

3.7	3.8		3.8
3.2	3.5		3.5
3.1	3.4		3.1
3.1	3.1		3.4

$\overline{T}_{a.in} = 29.3$ °C, $\overline{u}_{a.in} = 2.9$ m·s^{-1}

3.9	4.1		4.1
3.4	3.9		3.9
3.3	3.4		3.4
3.5	3.4		3.5

$\overline{T}_{a.in} = 29.8$ °C, $\overline{u}_{a.in} = 3.6$ m·s^{-1}

4.3	4.3		4.3
4.1	4.1		4.2
4.0	3.8		4.0
4.1	3.6		3.6

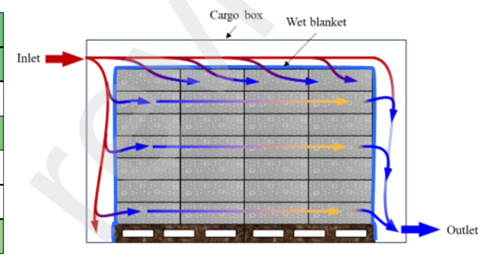

Fig. 7 Temperature differences (in °C) between the inlet air and the air in the different baskets in the middle plane for different air velocities. Time-averaged air and load surface temperatures were calculated over two hours during which temperature remained constant.

3.4 Simplified heat and mass transfer models for interpretation of load temperature evolution

A simplified one-dimensional heat and mass transfer models based on energy balance was devised to describe load temperature evolutions in a cargo chamber featuring a wet fabric blanket. As illustrated in **Fig. 8**, air flows through a channel between the wet fabric blanket and the chamber wall with external air above (T_{ext}). The load beneath the wet fabric blanket is characterized by a thickness $e = V/S$ where V denotes the load volume and S the load surface area. The load is in contact with the wet fabric blanket, which exposes to the flowing air. With each increment dx from 0 to L along the distance x, the contact area between air and load increases progressively from 0 to S due to the blanket swelling. Thus, the differential equations can be formulated in terms of dS rather than dx. As an initial approximation, the thermal inertia of the air and the wet fabric blanket are neglected in comparison to that of the load. Radiation heat exchange is also neglected due to the slight temperature differences between surfaces. Based on these presumptions, the heat and mass balances can be derived as follows.

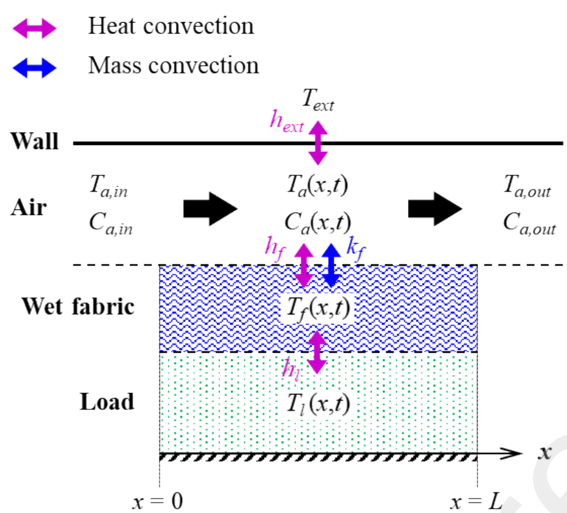

Fig. 8 1D simplified heat and mass transfer diagram.

It was assumed that the fabric blanket (temperature T_f) remained wet throughout the duration under consideration and it exchanges heat by convection with air (temperature T_a, moisture concentration C_a, heat transfer coefficient h_f) and with the load (temperature T_l, heat transfer coefficient h_l). Simultaneously, water evaporation flux from the fabric blanket into air (mass transfer coefficient k_f) can be represented by Eq. (10):

$$h_l(T_l - T_f) + h_f(T_a - T_f) = J_v L_v \tag{10}$$

where L_v is the latent heat of evaporation of water (J·kg^{-1}) and J_v is evaporation flux (kg·s^{-1}·m^{-2}) given by Eq. (11):

$$J_v = k_f(C_{sat}(T_f) - C_a) \tag{11}$$

where C_a is moisture concentration in air (kg·m^{-3}) and $C_{sat}(T_f)$ is saturated moisture concentration at the fabric blanket temperature. Approximately, the saturation moisture concentration can be determined by a second-degree polynomial function of the form: $C_{sat}(T_f) = c_1 + c_2T_f + c_3T_f^2$. The substitution of this polynomial function and Eq. (11) into Eq. (10) results in a simple equation to calculate the fabric blanket temperature Eq. (12).

$$\beta_1 T_f^2 + \beta_2 T_f + \beta_3 = 0 \tag{12}$$

where $\beta_1 = c_3 k_f L_v$, $\beta_2 = c_2 k_f L_v + h_l + h_f$ and $\beta_3 = (c_1 - C_a) k_f L_v - h_l T_l - h_f T_a$.

The air (volumetric flow rate $\dot{V}_a$) exchanges heat and water with the wet fabric blanket as previously mentioned and this air also exchanges heat with the external air (temperature T_{ext}, heat transfer coefficient h_{ext}):

$$\rho_a c_{pa} \dot{V}_a \frac{\partial T_a}{\partial S} = h_f (T_f - T_a) + h_{ext} (S_{ext}/S)(T_{ext} - T_a) \tag{13}$$

where S_{ext} is the surface of the cargo in contact with external air. Water evaporation flux increases the moisture concentration in the air, which can be expressed as:

$$\dot{V}_a \frac{\partial C_a}{\partial S} = J_v \tag{14}$$

The load temperature evolution can be then estimated from:

$$\rho_l c_{pl} e \frac{\partial T_l}{\partial t} = h_l (T_f - T_l) \tag{15}$$

Eqs. (10) to (15) can be solved numerically by space and time discretization. However, Eqs. (10) to (14) can be solved only by space discretization in two special cases of particular interest: the initial case where the load temperature is known and the equilibrium case where the load temperature reaches the fabric temperature. This allows notably to determine the fabric blanket temperatures (T_f) near the inlet and the outlet in the beginning and at equilibrium. In fact, T_f varies slightly and it can be assumed that T_f changes progressively from its initial value ($T_{f,0}$) to the equilibrium value ($T_{f,eq}$) with the same characteristic time (τ) as the load temperature evolution. Therefore, instead of solving directly Eqs. (10) to (15), it is possible to solve first Eqs. (10) to (14) for initial and equilibrium conditions. Then, Eq. (15) can be solved together with Eq (16):

$$T_f = T_{f,eq} + (T_{f,0} - T_{f,eq}) \exp(-t/\tau) \quad \text{where} \quad \tau = \frac{m_l c_{pl}}{h_l S} \tag{16}$$

The order of magnitude of the heat and mass transfer coefficients (h_l, h_f and k_f) were first approximated from the measured load temperature evolution. The air moisture concentration increased from inlet to outlet using heat and mass balances and assuming that T_f is close to the inlet bulk temperature.

For h_l: $$\frac{T_l - T_f}{T_{l0} - T_f} = \exp(-t/\tau) \quad \text{where} \quad \tau = \frac{m_l c_{pl}}{h_l S} \tag{17}$$

For k_f: $$\frac{C_{sat}(T_f) - C_{a,out}}{C_{sat}(T_f) - C_{a,in}} = \exp\left(-\frac{k_f S}{\dot{V}_a}\right) \tag{18}$$

Then, h_f can be estimated from the Lewis relation assuming that $h_f/k_f \cong \rho_a c_{pa}$ (Çengel and Ghajar, 2020). The external heat transfer coefficient (h_{ext}) of 10 W·m^{-2}·K^{-1} was assumed due to natural convection (Laguerre et al., 2012). The values of the input parameters used in the model are summarized in **Table 2**.

Table 2 Input parameters used in the model.

Input parameter	Symbol	Value	Reference
Regression coefficients	c_1 c_2 c_3	2.6880×10^{-5} 4.9010×10^{-5} 5.5957×10^{-3}	Fitting the saturation moisture concentration (C_{sat}) derived from saturation vapor pressure of water (p_{sat}) between 0 and 40 °C (Huang, 2018).
Molar mass, kg·mol^{-1} - Air - Water	 M_a M_v	 0.02897 0.018015	 Çengel et al. (2019) Çengel et al. (2019)
Universal gas constant, J·mol^{-1}·K^{-1}	R_u	8.31447	Çengel et al. (2019)
Latent heat of evaporation of water, kJ·kg^{-1}	L_v	2257	Çengel et al. (2019)
Specific heat capacity - Air - Polypropylene - Low-density polyethylene	 c_{pa} $c_{p,pp}$ $c_{p,pe}$	 1005 J·kg^{-1}·K^{-1} 1800 J·kg^{-1}·K^{-1} 2100 J·kg^{-1}·K^{-1}	 Çengel et al. (2019) Professional Plastics (2024) Professional Plastics (2024)
Heat transfer coefficient, W·m^{-2}·K^{-1} - External - Fabric - Load	 h_{ext} h_f h_l	 10 4.4, 6.7, and 10.5 at 0.8, 2.2, and 3.6 m·s^{-1}, respectively 1.6, 3.5, and 7.2 at 0.8, 2.2, and 3.6 m·s^{-1}, respectively	 Laguerre et al. (2012) Calculation using Eq. (17) Calculation using Eq. (18) and Lewis relation

Let SIH1 and the S4H7 in the middle plane represent the loads near the inlet and the outlet, respectively. To address the worst-case scenario (the warmest location where the product quality is the most impacted) and considering the significantly lower airflow velocities observed in weakly ventilated zones compared to near the inlet and short-circuit pathways (**Section 2.2.2**), the applied airflow rate was reduced to only 10% of the inlet airflow rate. A comparison between the calculated load temperature evolution (solid line) and the measured value (dot line) showed good agreement, as shown in **Fig. 9**. The mean relative error (MRE) between measured and calculated load temperature evolutions was calculated using Eq. (19) and the maximum value was 1.2%.

$$MRE(\%) = \frac{1}{N}\sum_{i=1}^{N}\left|\frac{x_{cal,i} - x_{exp,i}}{x_{exp,i}}\right| \times 100 \tag{19}$$

where x_{exp} and x_{cal} are measured and calculated values, respectively. N is number of measured data (N = 91 for each inlet velocity).

The simplified heat and mass transfer models developed in this study can be used to estimate the load temperature evolution near to the inlet and outlet, while the values of model input parameters are provided.

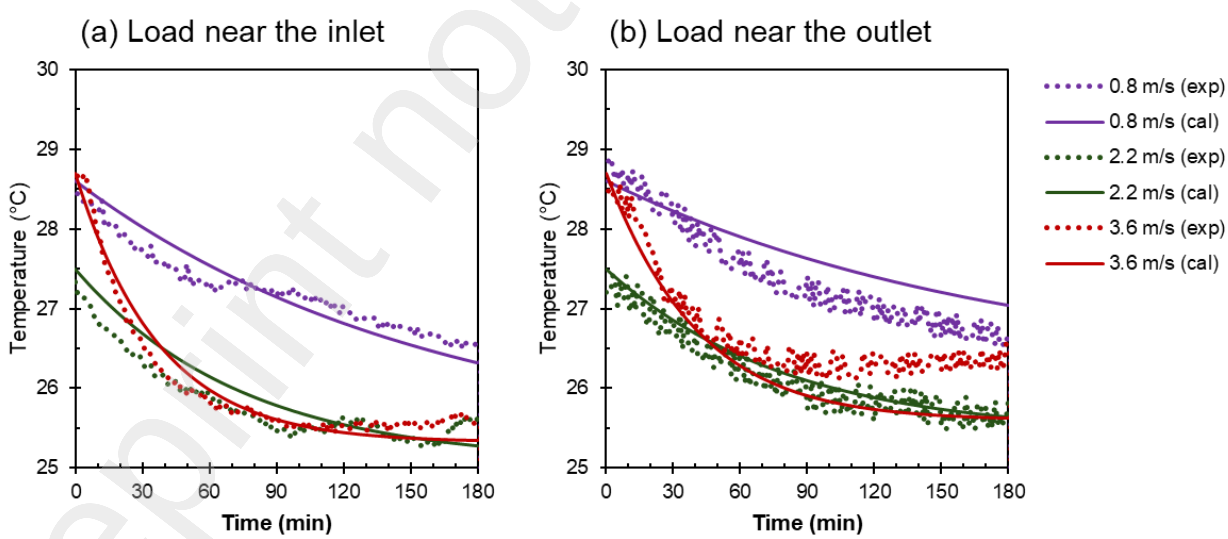

Fig. 9 Comparison between measured (dot line) and calculated (solid line) load temperature evolutions near (a) the inlet (S1H1) and (b) the outlet (S4H7) for three different inlet air velocity: 0.8, 2.2 and 3.6 m·s^{-1}.

3.5 Quality preservation performance

The performance of the EC system with the wet fabric blanket to preserve vegetable quality was investigated using lettuce as a case study. The inlet air velocity was maintained at 3.6 $m \cdot s^{-1}$ throughout the experiment. In the initial experiment (Exp. 1), time-averaged ambient air temperature and relative humidity were 28.8 ± 0.2 °C and 65.4 ± 2.8 %RH, respectively corresponding to the wet-bulb temperature of 23.8 ± 0.4 °C.

Fig. 10 illustrates the temperature variations of the products in various baskets on the left and the middle of the cargo chamber and outside considered as control. It was observed that the temperature of the products in all baskets decreased due to the EC effect. However, the temperature reduction rate varied with the basket positions in the chamber. As depicted in **Fig.10a** and **10b**, the products in the top baskets (S1H1 and S4H1) experienced the higher temperature decrease (4-5 °C) compared to those in the bottom baskets (S1H7 and S4H7, 2-3 °C). This discrepancy could be attributed to the higher air velocity around the top baskets compared to that around the bottom ones, as discussed in **Section 3.2**. Across all baskets within the cargo chamber, the product temperatures remained at least 2 °C lower than the ambient temperature for at least 17 hours (12 PM to 5 AM). This finding contrasts with that of Chopra et al. (2022), who observed that the temperature within the EC store was higher than the exterior temperature during nighttime temperature minima. This discrepancy may be attributed to the lower humidity conditions observed in our study.

The products in the baskets located outside the cargo chamber also exhibited a temperature decrease of about 1-2 °C during the initial 4 hours (**Fig. 10c**), gradually approaching the ambient temperature thereafter. This phenomenon could be attributed to water evaporation from the lettuce itself as evidenced by the results of mass loss, as presented **Fig. 11**.

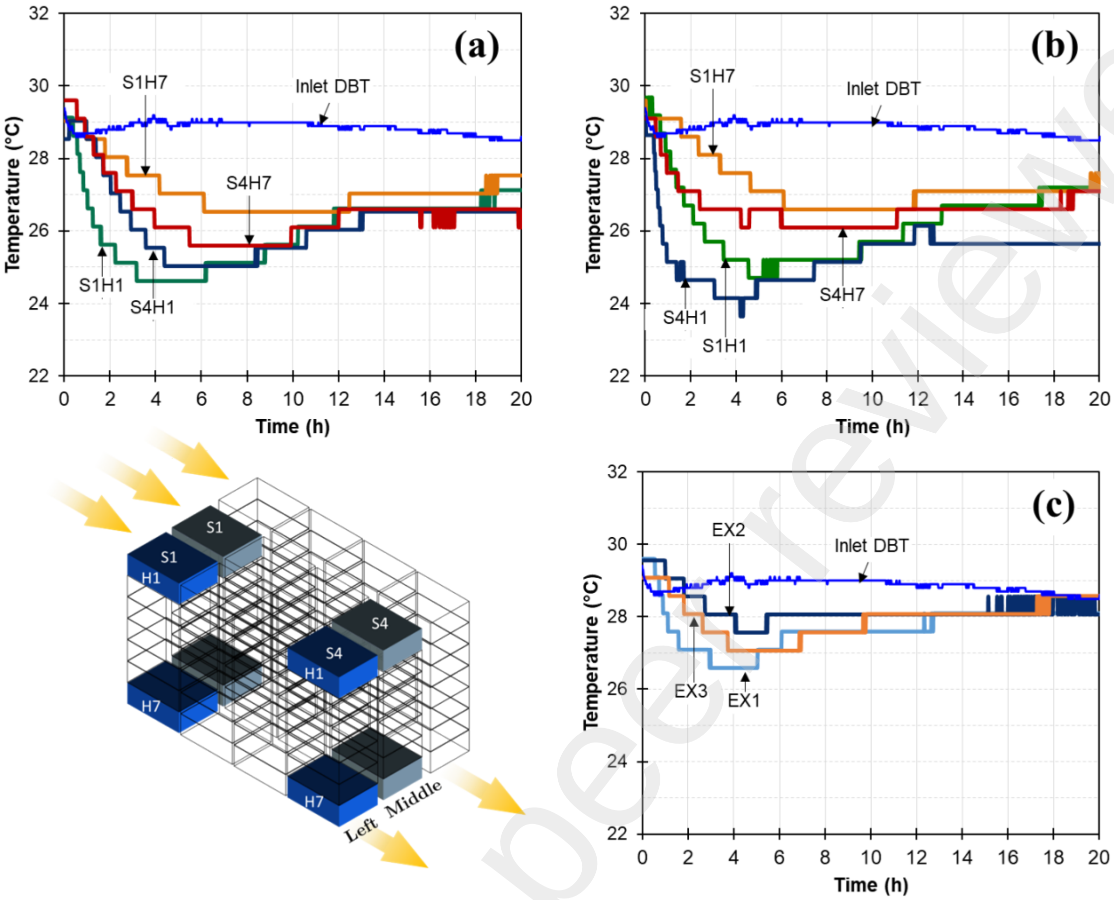

Fig. 10 Product temperature variations in various baskets: inside (a) on the left and (b) in the middle of the cargo chamber and (c) outside the cargo chamber. Indices of baskets (S#H#) refer to Fig. 5; DBT = Dry-Bulb Temperature.

The products kept inside the cargo chamber experienced a mass loss of less than 6%, whereas those placed outside the cargo chamber suffered almost 10% mass loss. The increase in the mass loss of leafy vegetables coincides closely with the loss of moisture content during storage. Typically, if a moisture loss exceeds 4%, it can lead to quality deterioration through wilting and shriveling, rendering the products unmarketable (Lufu et al., 2020). As depicted in **Fig. 11b**, the products kept inside the cargo chamber experienced a defective loss of 30-40%, while more than 50% of the products placed outside the cargo chamber were lost. As shown in **Fig. 12**, the baskets outside the cargo chamber contained more welted and limp lettuce than those inside the cargo chamber. The higher temperature in the basket outside the cargo chamber may elevate the respiration and transpiration rates of the vegetables and promote the growth of contaminated microorganisms. This led to greater levels of mass loss, defective loss, and undesirable appearance compared to the vegetables inside the cargo chamber. Based on the cumulative respired CO_2 calculated using Eq. (9), it was found that the cumulative respired CO_2 of products stored in the baskets inside the cargo (1.40×10^{-8} g·kg^{-1}, average of 8 baskets) was averagely 10% smaller than those outside the cargo chamber (1.55×10^{-8} g·kg^{-1}, average of 3 baskets). This suggests that the storage life of the products inside the cargo changed at a slower rate than those outside.

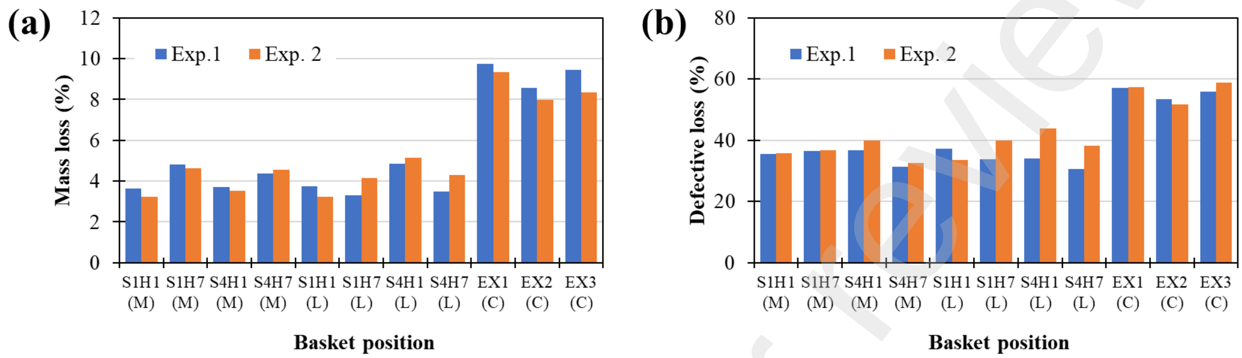

Fig. 11 Percentage of (a) mass loss and (b) defective losses of lettuce after kept inside and outside the cargo chamber for 20 hours. M = Baskets in the middle stack inside the cargo box; L = Baskets on the left stack inside the cargo box; C = Baskets outside of the cargo box (control).

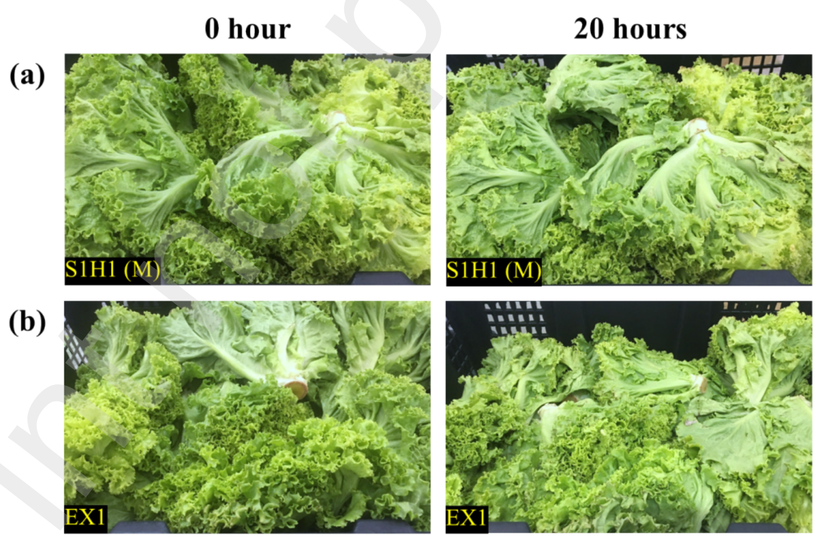

Fig. 12 Visual appearance of lettuce in the baskets after 20-h storage (a) inside and (b) outside the cargo chamber.

The experiment (Exp. 2) was repeated under the time-averaged ambient air temperature of 25.6 ± 0.2 °C and the relative humidity of 64.5 ± 2.9 %RH. The consistent results were obtained in terms of temperature reduction rate and product mass loss as shown in **Fig. 11**. These finding demonstrated that the EC system with the wet blanket has a potential to preserve vegetable quality during transportation.

4. Conclusions

The present experimental study investigated the EC performance in terms of both temperature reduction and product quality preservation utilizing a wet fabric blanket. The air and load surface temperatures were measured using calibrated T-type thermocouples and relative humidity by hygrometers. Under tropical climate conditions (29-30 °C and 70-75 %RH), this EC system demonstrated the capability to achieve at steady state a temperature reduction (air or load surface) of approximately 3.6-4.4 °C when operated with an inlet air velocity of 3.6 $m \cdot s^{-1}$. Furthermore, this EC system led to an increase in relative humidity ranging from 80% to 100%, resulting in a favorable impact on the freshness of horticultural produce. The influence of inlet air velocity on temperature reduction was also examined, revealing a decrease in temperature reduction as the inlet air velocity decreased. At the lowest inlet air velocity of 0.8 $m \cdot s^{-1}$, an air temperature reduction of approximately 2.4-3.4 °C was achieved. The simplified model of heat and mass transfers was developed allowing the estimation of load temperature evolution, which can be used by the stakeholders as an indicator of quality evolution.

The percentages of mass loss and defective loss of lettuce were measured after 20 hours of storage both inside and outside the cargo chamber. The results indicated that the mass loss for lettuce stored inside the cargo chamber ranged from 3-6%, whereas it ranged from 8-10% for lettuce stored outside. Similarly, the defective loss was lower for lettuce stored inside the cargo chamber, ranging from 30-40%, compared to more than 50% for lettuce stored outside. Moreover, the relative change in storage life of the products in the cargo chamber was about 10% slower.

The experimental data (temperature, humidity, product mass loss and defective losses) will be used to develop a quality model in a future study. The load temperature and quality models would be a useful numerical tool to predict the product quality at a sale point.

Overall, the findings of this study suggest the potential of using a wet blanket as an EC medium, offering a viable short-term solution to enhance cold chain logistics in Thailand before the establishment of a fully-fledged infrastructure.

Authorship contribution statement

Nattawut Chaomuang: Conceptualization, Methodology, Investigation, Formal analysis, Data Curation, Software, Writing - Original Draft, Visualization, Project administration, Funding acquisition,

Onrawee Laguerre: Formal analysis, Review & Editing, Supervision, **Suriyan Supapvanich:** Methodology, Formal analysis, Resources, Review & Editing, **Denis Flick:** Methodology, Formal analysis, Software, Review & Editing, **Steven Duret:** Methodology, Formal analysis, Review & Editing, Supervision.

Declaration of competing interest

No conflict of interest exists in the submission of this manuscript, and the manuscript is approved by all authors for publication. I would like to declare on behalf of my co-authors that the work described was original research that has not been published previously, and not under consideration for publication elsewhere, in whole or in part. All the authors listed have approved the manuscript that is enclosed.

Acknowledgements

This work was financially supported by Office of the Permanent Secretary, Ministry of Higher Education, Science, Research, and Innovation, Thailand, under the Research Grant for New Scholar (Grant No. RGNS-64-0244). The research was conducted as part of the INRAE-KU-KMITL-UPS Associated International Laboratory REWACT (REducing food WAste in cold Chain of Tropical countries).

References

Ambuko, J., Wanjiru, F., Chemining'wa, G., Owino, W., Mwachoni, E., 2017. Preservation of postharvest quality of leafy amaranth (Amaranthus spp.) vegetables using evaporative cooling. Journal of Food Quality 2017.

Çengel, Y.A., Boles, M.A., Kanoğlu, M., 2019. Thermodynamics: An engineering approach, 9 ed. McGraw-Hill Education, New York, NY.

Çengel, Y.A., Ghajar, A.J., 2020. Heat and mass transfer : fundamentals and applications. Mcgraw-Hill Education, New York, NY.

Chantarat, S., Attavanich, W., Sa-ngimnet, B., 2018. Microscopic view of Thailand's agriculture through the lens of farmer registration and census data, aBRIDGEd. Puey Ungphakorn Institute for Ecomonic Research.

Chaomuang, N., Flick, D., 2022. Potentials of wetted fabric as a cold medium for transport of horticultural products, 7th IIR International Conference on Sustainability and the Cold Chain Online. International Institute of Refrigeration, Online, p. 1116.

Chaomuang, N., Kosanlawat, K., Chitsuphap, N., Srithammasak, P., Krutharoj, S., 2023. Retaining quality of fresh Chinese kale (*Brassica oleracea*) during retailing at Thai wet markets by using an ice-cooled display cabinet, in: French Association of Refrigeration (Ed.), The 26th International Congress of Refrigeration (ICR 2023). International Institute of Refrigeration, Paris, France, pp. 77-86.

Chopra, S., Müller, N., Dhingra, D., Mani, I., Kaushik, T., Kumar, A., Beaudry, R., 2022. A mathematical description of evaporative cooling potential for perishables storage in India. Postharvest Biology and Technology 183, 111727.

Defraeye, T., Schudel, S., Shrivastava, C., Motmans, T., Umani, K., Crenna, E., Shoji, K., Onwude, D., 2022. The charcoal cooling blanket: A scalable, simple, self-supporting evaporative cooling device for preserving fresh foods. engrXiv (preprint).

Defraeye, T., Shoji, K., Schudel, S., Onwude, D., Shrivastava, C., 2023. Passive evaporative coolers for postharvest storage of fruit and vegetables: Where to best deploy them and how well do they perform. Frontiers in Food Science and Technology 3, 1100181.

DLT, 2022. Transport statistics report 2022. Department of Land Transport, Ministry of Transport.

DLT, 2023. Number of registered trucks for transport of chilled and frozen products. Department of Land Transport, Ministry of Transport.

Eriko, Y., Keiko, T., Daisuke, H., Wenzhong, H., Toshitaka, U., 2001. Effect of Temperature on the Respiration Rate of Some Vegetables. IFAC Proceedings Volumes 34, 205-210.

Guo, X., 2016. The mechanics of fiber-based absorbent evaporative cooling (fbaEC) for transport, Faculty of the Graduate School. University of Missouri, MO, USA.

Han, J.W., Zuo, M., Zhu, W.Y., Zuo, J.H., Lü, E.L., Yang, X.T., 2021. A comprehensive review of cold chain logistics for fresh agricultural products: Current status, challenges, and future trends. Trends in Food Science & Technology 109, 536-551.

Huang, J., 2018. A Simple Accurate Formula for Calculating Saturation Vapor Pressure of Water and Ice. Journal of Applied Meteorology and Climatology 57, 1265-1272.

IIR, 2020. The role of refrigeration in worldwide nutrition. 6th Informatory Note on Refrigeration and Food.

Kim, W.R., Aung, M.M., Chang, Y.S., Makatsoris, C., 2015. Freshness Gauge based cold storage management: A method for adjusting temperature and humidity levels for food quality. Food Control 47, 510-519.

Kwanmuang, K., Pongputhinan, T., Jabri, A., Chitchumnung, P., 2020. Small-scale farmers under Thailand's smart farming system. FFTC-AP, 2647.

Laguerre, O., Hoang, M.H., Flick, D., 2012. Heat transfer modelling in a refrigerated display cabinet: The influence of operating conditions. Journal of Food Engineering 108, 353-364.

Liu, Q., Guo, C., Ma, X., You, Y., Li, Y., 2020. Experimental study on total heat transfer efficiency evaluation of an indirect evaporative cooler. Applied Thermal Engineering 174, 115287.

Lufu, R., Ambaw, A., Opara, U.L., 2020. Water loss of fresh fruit: Influencing pre-harvest, harvest and postharvest factors. Scientia Horticulturae 272, 109519.

Mahangade, P.S., Mani, I., Beaudry, R., Müller, N., Chopra, S., 2020. Using Amaranth as a Model Plant for Evaluating Imperfect Storages: Assessment of Solar-refrigerated and Evaporatively-cooled Structures in India. HortScience horts 55, 1759-1765.

Nkolisa, N., Magwaza, L.S., Workneh, T.S., Chimphango, A., 2018. Evaluating evaporative cooling system as an energy-free and cost-effective method for postharvest storage of tomatoes (Solanum lycopersicum L.) for smallholder farmers. Scientia Horticulturae 241, 131-143.

Professional Plastics, 2024. Thermal properties of plastic materials.

Sathapongpakdee, P., 2022. Thailand industry outlook 2022-24: Road freight transportation service, Krungsri Research. Bank of Ayudhya, pp. 1-22.

Sensirion, 2009. Introduction to Humidity: Basic Principles on Physics of Water Vapor. Sensirion, The Sensor Company.

Stull, R., 2011. Wet-bulb temperature from relative humidity and air temperature. Journal of applied meteorology and climatology 50, 2267-2269.

Tejero-González, A., Franco-Salas, A., 2021. Optimal operation of evaporative cooling pads: A review. Renewable and Sustainable Energy Reviews 151, 111632.

TMD, 2020. The Climate of Thailand. Thai Meteorological Department, Ministry of Digital Economy and Society.

Vala, K.V., Joshi, D.C., 2010. Development of evaporative cooling transportation system for perishable commodities. Journal of Agricultural Engineering 47, 27-33.

Xuan, Y., Xiao, F., Niu, X., Huang, X., Wang, S., 2012. Research and application of evaporative cooling in China: A review (I)–Research. Renewable and Sustainable Energy Reviews 16, 3535-3546.